

An Exact Solution for Classic Coupled Magneto-Thermo-Elasticity in Cylindrical Coordinates

M. Jabbari^{1,*}, H. Dehbani²

¹Postgraduate School, South Tehran Branch, Islamic Azad University, Tehran, Iran

²Sama technical and vocational training college, Islamic Azad University, Varamin Branch, Varamin, Iran

Received 8 November 2011; accepted 7 January 2012

ABSTRACT

In this paper, the classic coupled Magneto-thermo-elasticity model of hollow and solid cylinders under radial-symmetric loading condition (r, t) is considered. A full analytical and the direct method based on Fourier Hankel series and Laplace transform is used, and an exact unique solution of the classic coupled equations is presented. The thermal and mechanical boundary conditions, the body force, the heat source and magnetic field vector are considered in the most general forms, where no limiting assumption is used. This generality allows to simulate a variety of applicable problems. The results are presented for thermal and mechanical shock, separately, and compare the effect of magnetic field on temperature and displacement.

© 2012 IAU, Arak Branch. All rights reserved.

Keywords : Coupled magneto –thermo-elasticity; Hollow cylinder; Exact solution

1 INTRODUCTION

IN recent years, coupled thermoelasticity has developed enormously because there are many applications of it in industries related to advanced design such as aerospace, turbines, jet motors, nuclear reactors, etc. Therefore it is crucial to regard the deformation and temperature distributions in thermal shock cases. In coupled problems of thermoelasticity take into account the time rate of change of the first variation invariant of strain tensor in the first law of thermodynamics causes the coupling between elastic and thermal field. The mathematical treatment of coupled thermoelasticity problems by analytical methods is rather complicate so that only very basic problems have been treated in the literature and many works have been done by numerical methods of solution for coupled Magneto-thermo-elasticity problems.

There are some few papers that presented the closed-form or analytical solution for coupled cases. Hetnarski [1] found the solution of coupled thermoelasticity in the form of series function. Hetnarski and Ignaczak [2] presented a study of the one-dimensional thermoelastic waves produced by an instantaneous plane source of heat in homogeneous isotropic infinite and semi-infinite bodies of the Green-Lindsay type. Also these authors presented an analysis of laser-induced waves propagating in an absorbing thermoelastic semi-space of the Green-Lindsay type [3]. Georgiadis and Lykotrafitis obtained a three-dimensional transient thermoelastic solution for Rayleigh-type disturbances propagating on the surface of a halfspace [4]. Wagner [5] presented the fundamental matrix of a system of partial differential operators that governs the diffusion of heat and the strains in elastic media. This method can be used to predict temperature distribution and the strains by an instantaneous point heat point source of heat or by a suddenly applied delat force.

*Corresponding author. Tel.: +98 21 22217158 ; Fax: +98 21 22211088
E-mail address: mohsen.jabbari@gmail.com (M. Jabbari).

Majority of papers focused on numerical methods in coupled problems. Lee [6] considered the problem of three-dimensional axisymmetric quasi-static coupled magneto-thermoelasticity for the laminated circular conical shells subjected to magnetic and temperature fields. Laplace transform and finite difference methods are used to analyze the problem. He obtained solutions for the temperature and thermal deformation distributions in a transient and steady state. Dai and Fu [7] considered the magneto-thermoelastic problem of functionally graded material (FGM) hollow structures subjected to mechanical loads. The material stiffness, the thermal expansion coefficient and the magnetic permeability are assumed to obey the simple power-law variation through the structures' wall thickness. The aim of their research was to understand the effect of composition on magneto-thermoelastic stresses and to design optimum FGM hollow cylinders and hollow spheres. Wang and Dong [8] presented theoretical methods for analyzing magneto-thermoelastic responses and perturbation of the magnetic field vector in a conducting non-homogeneous thermoelastic cylinder subjected to thermal shock. By making use of finite Hankle integral transforms, the analytical expressions for magneto-thermodynamic stress and perturbation response of an axial magnetic field vector in a non-homogeneous cylinder are obtained. Dai and Wang [9] presented an analytical method to solve the problem for the dynamic stress-focusing and centred-effect of perturbation of the magnetic field vector in orthotropic cylinders under thermal and mechanical shock loads. Analytical expressions for the dynamic stresses and the perturbation of the magnetic field vector are obtained by means of finite Hankel transforms and Laplace transforms.

Misra et al. [10] considered the problem of a half-space under the influence of an external primary magnetic field and an elevated temperature field arising out of a ramp-type heating of the surface. It is found that the stress distribution and the secondary magnetic field are almost independent of thermal relaxation time, but are significantly dependent on the mechanical relaxation time. Massalas [11] considered the phenomenological description of the magneto-thermoelastic interactions in ferromagnetic material in the framework of the generalized theory of thermoelasticity proposed by Green and Laws.

The material is supposed to be homogeneous, anisotropic and elastic undergoing large deformations. The analysis is based on the thermodynamic laws of quasi-magnetostatics. Misra et al. [12] presented a solution for the induced temperature and stress fields in an infinite transversely isotropic solid continuum with a cylindrical hole using the integral transform. The solid medium is considered to be exposed to a magnetic field and the cavity surface is assumed to be subjected to a ramp-type heating. Green and Lindsay model is used to account for finite velocity of heat conduction. Roy Choudhuri and Roy Chatterjee [13] presented the propagation of magneto-thermoelastic disturbances produced by a thermal shock in a finitely conducting elastic half-space in contact with a vacuum, they used Laplace transform. The temperature-rate dependent theory of thermoelasticity proposed by Green and Lindsay is employed. It is found that the temperature and deformation are discontinuous at the wave fronts whereas the perturbed magnetic fields suffer delta function singularity at these locations. Paul and Narasimhan [14] studied the problem of axisymmetric axial stress wave generation in a thermoelastic circular cylindrical bar in the presence of an applied magnetic field. It is assumed that the surface of the cylinder is free from mechanical loadings and thermal radiation. A general solution is obtained by perturbation technique and is annihilated to a particular case where in the applied magnetic field is constant in space and time. Roy Chatterjee and Roychoudhuri [15] presented the magneto-thermoelastic disturbances in a perfectly electrically conducting elastic half-space, in contact with a vacuum, due to a thermal shock applied on the plane boundary of the half-space. The theory of thermoelasticity proposed by Green and Lindsay is used to account for the interaction between the elastic and thermal fields. Maruszewsk [16] presented the nonlinear magneto-thermoelastic equations in soft ferromagnetic and elastic bodies. The symmetry of couplings in these equations is also investigated. Magdy et al. [17] presented the equations of magneto-thermoelasticity with two relaxation times and with variable electrical and thermal conductivity for one-dimensional problems including heat sources that are cast into matrix form, using the state space and Laplace transform techniques. The resulting formulation is applied to a problem for the whole conducting space with a plane distribution of heat sources. Chen and Lee [18] worked on magneto-thermoelasticity by introducing two displacement functions and two stress functions. The governing equations of the linear theory of magneto-electro-thermo-elasticity with transverse isotropy are simplified. The material inhomogeneity along the axis of symmetry can be taken into account and an approximate laminate model is employed to facilitate deriving analytical solutions. Tianhu et al. [19] reported the theory of generalized thermoelasticity, based on the theory of Lord and Shulman with one relaxation time, used to study the electromagneto-thermoelastic interactions in a semi-infinite perfectly conducting solid subjected to a thermal shock on its surface when the solid and its adjoining vacuum is subjected to a uniform axial magnetic field. He used Laplace transform. The Maxwell's equations are formulated and the generalized electromagneto-thermoelastic coupled governing equations are established. Sharma and pal [20] investigated the propagation of magnetic-thermoelastic plane wave in an initially unstressed, homogeneous isotropic conducting plate under uniform static magnetic field. The generalized theory of thermoelasticity is employed by

assuming the electrical behaviour as quasi-static and the mechanical behaviour as dynamic. At short wavelength limits, the secular equations for symmetric and skew-symmetric modes reduce, to Rayleigh surface wave frequency equation, because a finite thickness plate in such a situation behaves like a semi-infinite medium. Abd-Alla et al. [21] have investigated the stress, temperature, and magnetic field in an isotropic homogeneous viscoelastic medium with a spherical cavity in a primary magnetic field, when the curved surface of the spherical cavity subjected to periodic loading. The generalized theory of thermoelasticity proposed by Green and Lindsay elasticity is applied to account for finite velocity of heat propagation.

In this work, a full analytical method is proposed to obtain the response of the governing equations of the classical coupled magneto thermoelasticity in cylindrical coordinates, where an exact solution is presented. The method of solution is based on the Fourier expansion and eigenfunction methods, which is a traditional and routine method in solving the partial differential equations. Since the coefficients of equations are not functions of the time variable (t), an exponential form is considered for the general solution. For the particular solution, that is, the response to mechanical and thermal shocks and magnetic field vector, the eigenfunction method and Laplace transformation are used.

This work is the extension of the previous paper of [22].

2 GOVERNING EQATIONS

A hollow cylinder with inner and outer radius r_i and r_o made of isotropic material subjected to the radial-symmetric mechanical, thermal shock loads and magnetic field vector is considered. The classical theory of coupled magneto thermoelasticity for the wave propagation is considered. If u is the displacement component in the radial direction, the strain-displacement relations for the radial-symmetric loading conditions are [30]:

$$\varepsilon_{rr} = u_{,r} \quad \varepsilon_{\theta\theta} = \frac{u}{r} \quad (1)$$

where $(,)$ denotes partial derivative.

The stress-strain relations for plane strain conditions are[30]:

$$\begin{aligned} \sigma_{rr} &= \frac{E}{(1+\nu)(1-2\nu)} [(1-\nu)\varepsilon_{rr} + \nu\varepsilon_{\theta\theta}] - \frac{E\alpha}{(1-2\nu)} T(r,t) \\ \sigma_{\theta\theta} &= \frac{E}{(1+\nu)(1-2\nu)} [\nu\varepsilon_{rr} + (1-\nu)\varepsilon_{\theta\theta}] - \frac{E\alpha}{(1-2\nu)} T(r,t) \end{aligned} \quad (2)$$

where σ_{ij} and ε_{ij} ($i, j = r, \theta$) are the radial and hoop stresses and strain tensor, respectively; $T(r,t)$ is the temperature distribution, α is the coefficient of thermal expansion, E is the modulus of elasticity and ν is the Poisson's ratio.

Assuming that the magnetic permeability, μ , hollow cylinder is equal to the magnetic permeability of the medium around it, and also the medium is non-ferromagnetic and non-ferroelectric and ignoring the Thompson effect, the simplified Maxwell's equations of electrodynamics for a perfectly conducting elastic medium are [7]:

$$\begin{aligned} \vec{J} &= \nabla \times \vec{h} & h &= \nabla \times (\vec{U} \times \vec{H}) \\ \text{div} h &= 0 & \tau_z &= \mu(\vec{J} \times \vec{H}) \end{aligned} \quad (3)$$

Applying an initial magnetic field vector $H(0,0,H_z)$ in cylindrical coordinates to Eq. (3), yields [7]:

$$\begin{aligned}\vec{U} &= (u, 0) & \vec{h} &= (0, 0, h_z) \\ h_z &= -H_z \left(u_r + \frac{u}{r} \right) & \tau_z &= \mu (\vec{J} \times \vec{H}) = \mu H_z^2 \left(u_r + \frac{u}{r} \right)\end{aligned}\quad (4)$$

where τ_z , μ , \vec{H} , \vec{J} and \vec{h} are electro-magnetic stress (N/m^2), magnetic permeability (H/m), magnetic intensity vector, electric current density vector and perturbation of magnetic field vector, respectively.

The equation of motion in the radial direct is [30]:

$$\sigma_{rr,r} + \frac{1}{r}(\sigma_{rr} - \sigma_{\theta\theta}) + \frac{\partial \tau_z}{\partial r} + F(r, t) = \rho \ddot{u} \quad (5)$$

where $F(r, t)$ is body force in the radial direction Fig 1.

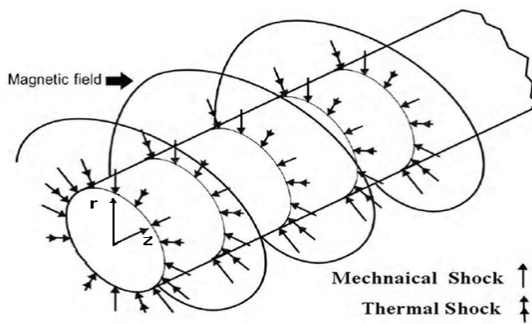


Fig.1

The geometry of a cylinder under a magnetic field, Mechanical and thermal shock

Using the relations (1) to (5), the Navier equation in term of the displacement components is obtained as:

$$\begin{aligned}u_{,rr} + \frac{1}{r}u_{,r} - \frac{1}{r^2}u - \frac{(1+\nu)}{(1-\nu)}\alpha T_{,r}(r, t) + \frac{(1+\nu)(1-2\nu)}{(1-\nu)E}\mu H_z^2 \left\{ u_{,rr} + \frac{1}{r}u_{,r} - \frac{1}{r^2}u \right\} \\ - \frac{(1+\nu)(1-2\nu)}{E(1-\nu)}\rho \ddot{u} = -F(r, t)\end{aligned}\quad (6)$$

The coupled heat conduction equation for the radial-symmetric loading condition is [30] :

$$T_{,rr} + \frac{1}{r}T_{,r} - \frac{\rho c}{k}\dot{T} - \frac{E\alpha}{k(1-2\nu)}T_o \left(\dot{u}_{,r} + \frac{1}{r}\dot{u} \right) = -\frac{Q(r, t)}{K} \quad (7)$$

where k , ρ , c , T_o and $Q(r, t)$ are the thermal conduction coefficient, the density, the specific heat, initial temperature and heat generation source. Mechanical and thermal boundary conditions are [29]:

$$\begin{aligned}C_{11}u(r_i, t) + C_{12}u_{,r}(r_i, t) + C_{12}T(r_i, t) &= f_1(r) \\ C_{12}u(r_o, t) + C_{22}u_{,r}(r_o, t) + C_{23}T(r_o, t) &= f_2(r) \\ C_{31}T(r_i, t) + C_{32}T_{,r}(r_i, t) &= f_3(r) \\ C_{41}T(r_o, t) + C_{42}T_{,r}(r_o, t) &= f_4(r)\end{aligned}\quad (8)$$

where C_{ij} are the mechanical and thermal coefficients, r_i and r_o are inner and outer radius respectively. By assigning different values for them, types of mechanical and thermal boundary conditions may be obtained. These boundary conditions include the displacement, strain, stress, specified temperature, convection, and heat flux. The initial boundary conditions are assumed in general form [22-28]:

$$\begin{aligned} U(r, 0) &= f_5(r) \\ \dot{U}(r, 0) &= f_6(r) \\ T(r, 0) &= f_7(r) \end{aligned} \tag{9}$$

3 SOLUTION

Eqs. (6) and (7) are the system of nonhomogeneous partial differential equations with nonconstant coefficients (functions of radius variable r) and with general and particular solutions.

3.1 General solution with homogeneous boundary conditions

Since the coefficients of these equations are independent of time variable (t), the exponential function form of the time variable may be assumed for the general solution as [22-28]:

$$u(r, t) = [U(r)] e^{\lambda t} \qquad T(r, t) = [\theta(r)] e^{\lambda t} \tag{10}$$

where λ is eigenvalue and show the natural frequency. Substituting Eq. (10) into homogeneous pares of Eqs. (6) and (7), yields:

$$\begin{aligned} u'' + \frac{1}{r}u' - \frac{1}{r^2}u + d_1\theta' + d_2\lambda^2u + d_5 \left(u'' + \frac{1}{r}u' - \frac{1}{r^2}u \right) &= 0 \\ \theta'' + \frac{1}{r}\theta' + d_3\lambda\theta + d_4\lambda \left(u' + \frac{1}{r}u \right) &= 0 \end{aligned} \tag{11}$$

Eqs.(11) are system of ordinary differential equations, where the prime symbol (') shows differentiation with respect to the radius variable (r) and d_1 - d_5 are constant parameters given in appendix .

The first solutions of $U_1(r)$ and $\theta_1(r)$ are considered as [22-28]:

$$U_1(r) = A_1J_1(\beta r) \qquad \theta_1(r) = B_1J_0(\beta r) \tag{12}$$

where β shows nodal lines in natural vibrating modes and A_1 and B_1 are the maximum amplitudes. Substituting Eq. (12) in Eq. (11), and using the formulas for derivatives of the Bessel function, such as $dJ_n(\beta r)/dr = \beta J_{n-1}(\beta r) - n(J_n(\beta r)/r)$, yields:

$$\begin{aligned} \{(-1+d_5)\beta^2 + d_2\lambda^2\}A_1 - B_1d_1\beta\} J_1(\beta r) &= 0 \\ \{\lambda d_4\beta A_1 + (-\beta^2 + \lambda d_3)B_1\} J_0(\beta r) &= 0 \end{aligned} \tag{13}$$

Eq. (13) shows U_1 and θ_1 can be the solution of Eqs. (11), if only and if:

$$\begin{bmatrix} -(1+d_5)\beta^2 + d_2\lambda^2 & -d_1\beta \\ \lambda d_4\beta & -\beta^2 + \lambda d_3 \end{bmatrix} \times \begin{Bmatrix} A_1 \\ B_1 \end{Bmatrix} = \begin{Bmatrix} 0 \\ 0 \end{Bmatrix} \tag{14}$$

The nontrivial solution of Eq. (14) is obtained by setting the determinant of this equation equal to zero as:

$$(-(1+d_5)\beta^2 + \lambda^2 d_2)(-\beta^2 + \lambda d_3) + d_1 d_4 \beta^2 \lambda = 0 \tag{15}$$

Eq.(15) is the first characteristic equation. Thus, it is concluded that the first solution for U_1 and θ_1 satisfy the system of Eq.(11), and they are the first solutions of this system.

The second solution of the system of ordinary differential equations with nonconstant coefficients Eq. (11) must be considered as [22-28]:

$$\begin{aligned} U_2(r) &= [A_2 J_1(\beta r) + A_3 r J_2(\beta r)] \\ \theta_2(r) &= [B_2 J_0(\beta r) + B_3 r J_1(\beta r)] \end{aligned} \quad (16)$$

Substituting Eq. (16) to Eq. (11) yields:

$$\begin{aligned} &\{((1+d_5)\beta^2 - \lambda^2 d_2)A_3 + d_1 \beta B_3\} r J_0(\beta r) + \\ &\left\{ -(1+d_5)\beta^2 - \lambda^2 d_2 \right\} A_2 + \lambda^2 d_2 \frac{2}{\beta} A_3 - d_1 \beta B_2 \left\} J_1(\beta r) = 0 \right. \\ &\left\{ A_2 \lambda d_4 \beta + (-\beta^2 + \lambda d_3) B_2 + 2\beta B_3 \right\} J_0(\beta r) \\ &+ \left\{ A_3 \lambda d_4 \beta (-\beta^2 + \lambda d_3) B_3 \right\} r J_1(\beta r) = 0 \end{aligned} \quad (17)$$

The expressions for U_2 and θ_2 can be the solution of Eqs. (11), if only and if:

$$\begin{bmatrix} -(1+d_5)\beta^2 + \lambda^2 d_2 & -d_1 \beta \\ \lambda d_4 \beta & (-\beta^2 + \lambda d_3) \end{bmatrix} \begin{Bmatrix} A_3 \\ B_3 \end{Bmatrix} = \begin{Bmatrix} 0 \\ 0 \end{Bmatrix} \quad (18)$$

$$\left\{ -(1+d_5)\beta^2 + \lambda^2 d_2 \right\} A_2 + \lambda^2 d_2 \frac{2}{\beta} A_3 - d_1 \beta B_2 = 0 \quad (19)$$

$$\left\{ \lambda d_4 \beta A_2 + (-\beta^2 + \lambda d_3) B_2 + 2\beta B_3 \right\} = 0 \quad (20)$$

The nontrivial solution of Eqs. (18) is obtained by setting the determinant equal to zero as:

$$(-(1+d_5)\beta^2 + \lambda^2 d_2)(-\beta^2 + \lambda d_3) + d_1 d_4 \beta^2 \lambda = 0 \quad (21)$$

The characteristic Eq.(21) is the same as the characteristic Eq. (15). This equality is interesting as it prevents mathematical dilemma and complexity, and a single value for the eigenvalue β simultaneously satisfies both characteristic Eqs. (15) and (21). Eqs.(19) and (20) give the relation between A_2 , A_3 , B_2 , and B_3 , and they play as the balancing ratios that help Eq. (16) to be the second solution of the system of Eq. (11). Eqs. (19) and (20) are two algebraic equations with six unknown A_2 , A_3 , B_2 , B_3 , β and λ . Since the number of unknowns is more than the equations, there is no restriction to bring noncompatibility between Eqs. (18) – (20). The complete general solutions for the solid cylinder are [22-28]:

$$\begin{aligned} u^s(r) &= A_1 J_1(\beta r) + A_2 [J_1(\beta r) + \zeta_1 r J_2(\beta r)] \\ \theta^s(r) &= A_1 \zeta_2 J_0(\beta r) + A_2 [\zeta_3 J_0(\beta r) + \zeta_4 r J_1(\beta r)] \end{aligned} \quad (22)$$

Those for hollow cylinder are:

$$\begin{aligned} U^s(r) &= A_1 J_1(\beta r) + A_2 [J_1(\beta r) + \zeta_1 r J_2(\beta r)] + A_3 Y_1(\beta r) + A_4 [Y_1(\beta r) + \zeta_1 r Y_2(\beta r)] \\ \theta^s(r) &= A_1 \zeta_2 J_0(\beta r) + A_2 [\zeta_3 J_0(\beta r) + \zeta_4 r J_1(\beta r)] + A_3 \zeta_2 Y_0(\beta r) + A_4 [\zeta_3 Y_0(\beta r) + \zeta_4 r Y_1(\beta r)] \end{aligned} \quad (23)$$

where $\zeta_1 - \zeta_4$ are ratios obtained from Eqs. (14), (19) and (20) and are given in appendix. Substitute U^g and θ^g in homogeneous form of boundary conditions Eq.(8) , four linear algebraic equations are obtained as:

$$\begin{bmatrix} \mu_{11} & \mu_{12} & \mu_{13} & \mu_{14} \\ \mu_{21} & \mu_{22} & \mu_{23} & \mu_{24} \\ \mu_{31} & \mu_{32} & \mu_{33} & \mu_{34} \\ \mu_{41} & \mu_{42} & \mu_{43} & \mu_{44} \end{bmatrix} \begin{Bmatrix} A_1 \\ A_2 \\ A_3 \\ A_4 \end{Bmatrix} = \begin{Bmatrix} 0 \\ 0 \\ 0 \\ 0 \end{Bmatrix} \quad (24)$$

where μ_{ij} are the coefficients depending on β and λ and are given in appendix. Setting the determinant of coefficients of Eq. (24) equal to zero, the second characteristic equation is obtained. A simultaneous solution of this equation and Eq. (15), result in an infinite number of tow eigenvalues, β_n and λ_n . Therefore U^g and θ^g are rewritten as [22-28]:

$$\begin{aligned} U^g(r) &= A_1 \left[J_1(\beta_n r) + [\zeta_5 J_1(\beta_n r) + \zeta_6 r J_2(\beta_n r)] + \zeta_7 Y_1(\beta_n r) + [\zeta_8 Y_1(\beta_n r) + \zeta_9 r Y_2(\beta_n r)] \right] \\ \theta^g(r) &= A_1 \left[\zeta_{10} J_0(\beta_n r) + [\zeta_{11} J_0(\beta_n r) + \zeta_{12} r J_1(\beta_n r)] + \zeta_{13} Y_0(\beta_n r) + [\zeta_{14} Y_0(\beta_n r) + \zeta_{15} r Y_1(\beta_n r)] \right] \end{aligned} \quad (25)$$

where $\zeta_5 - \zeta_{15}$ are eigenvectors can be obtained from Eqs (24). Let us show the functions in the brackets of Eqs. (25) by functions H_1 and H_0 as:

$$\begin{aligned} H_1(\beta_n r) &= J_1(\beta_n r) + [\zeta_5 J_1(\beta_n r) + \zeta_6 r J_2(\beta_n r)] + \zeta_7 Y_1(\beta_n r) + [\zeta_8 Y_1(\beta_n r) + \zeta_9 r Y_2(\beta_n r)] \\ H_0(\beta_n r) &= \zeta_{10} J_0(\beta_n r) + [\zeta_{11} J_0(\beta_n r) + \zeta_{12} r J_1(\beta_n r)] + \zeta_{13} Y_0(\beta_n r) + [\zeta_{14} Y_0(\beta_n r) + \zeta_{15} r Y_1(\beta_n r)] \end{aligned} \quad (26)$$

According to the Sturm-Liouville theories, these functions are orthogonal with respect to the weight function $p(r) = r$ as [22-28]:

$$\int_{r_i}^{r_o} H(\beta_n r) H(\beta_m r) r dr = \begin{cases} 0 & n \neq m \\ \|H(\beta_n r)\|^2 & n = m \end{cases} \quad (27)$$

where $\|H(\beta_n r)\|$ is norm of the H function and equals [22-28]:

$$\|H(\beta_n r)\| = \left[\int_{r_i}^{r_o} r H^2(\beta_n r) dr \right]^{\frac{1}{2}} \quad (28)$$

Due to the orthogonality of function H, every piecewise continuous function, such as $f(r)$ can be expanded in terms of the function H (either for H_1 or H_0), and is called the H-Fourier series as [22,23]:

$$f(r) = \sum_{n=1}^{\infty} e_n H(\beta_n r) \quad (29)$$

where e_n equals:

$$e_n = \frac{1}{\|H(\beta_n r)\|^2} \int_{r_i}^{r_o} f(r) H(r) r dr \quad (30)$$

There are three groups for eigenvalues λ_n , where the first λ_{n1} is real and negative, and the second and third ones,

λ_{n2} and λ_{n3} , are conjugate complex with a negative real part, $-\xi_n \omega_n$, and an imaginary part, $\pm \omega_{dn}$. Terms ω_{dn} and ω_n are the damped and nondamped thermal-mechanical natural frequencies, and ξ_n is the damping ratio for the nth natural mode. Eq. (15) is an algebraic equation in polynomial form, and the determinant of Eq. (24) is an algebraic equation in the Bessel function form. The exact analytical solution for this system of nonlinear algebraic equations is complicated, and the numerical method of solution is employed in this paper. Since the Bessel functions are periodic, the system has an infinite number of roots.

Using Eqs. (10), (25), and (26), the displacement and temperature distributions due to the general solution become [22-28]:

$$\begin{aligned} u^g(r, t) &= \sum_{n=1}^{\infty} \left\{ \sum_{m=1}^3 a_{nm} e^{\lambda_{nm} t} \right\} H_1(\beta_n r) \\ T^g(r, t) &= \sum_{n=1}^{\infty} \left\{ \sum_{m=1}^3 N_{nm} e^{\lambda_{nm} t} \right\} H_0(\beta_n r) \end{aligned} \quad (31)$$

Using initial conditions Eq.(9) and with the help of Eqs. (6)and (7)and(29)to(31), unknown constants, a_{nm} , N_{nm} are obtained.

3.2 Particular solution with non-homogeneous boundary conditions

The general solutions may be used as proper functions to guess the particular solution adopted to the nonhomogeneous parts of Eqs. (6) and (7) and the nonhomogeneous boundary conditions Eq. (8) as [22-28]:

$$\begin{aligned} u^p(r, t) &= \sum_{n=1}^{\infty} \left\{ [G_{1n}(t)J_1(\beta_n r) + G_{2n}(t)rJ_2(\beta_n r)] + r^2 G_{3n}(t) \right\} \\ T^p(r, t) &= \sum_{n=1}^{\infty} \left\{ [G_{3n}(t)J_0(\beta_n r) + G_{4n}(t)rJ_1(\beta_n r)] + r^2 G_{6n}(t) \right\} \end{aligned} \quad (32)$$

For solid cylinder, the second type of Bessel function Y is excluded. It is necessary and suitable to expand the body force $F(r,t)$ and heat source $Q(r,t)$ in the H-Fourier expansion form as [22-28]:

$$\begin{aligned} F(r, t) &= \sum_{n=1}^{\infty} F_n(t)H_1(\beta_n r) \\ Q(r, t) &= \sum_{n=1}^{\infty} Q_n(t)H_0(\beta_n r) \end{aligned} \quad (33)$$

where $F_n(t)$ and $Q_n(t)$ are

$$\begin{aligned} F_n(t) &= \frac{1}{\|H_1(\beta_n r)\|^2} \int_{r_i}^{r_o} F(r, t)H_1(\beta_n r)rdr \\ Q_n(t) &= \frac{1}{\|H_0(\beta_n r)\|^2} \int_{r_i}^{r_o} Q(r, t)H_0(\beta_n r)rdr \end{aligned} \quad (34)$$

Substituting Eqs.(32) and (33) into nonhomogeneous form of Eq. (6) and (7) yields:

$$\left\{ \begin{aligned} &-(1+d_5)G_1(t)\beta^2 + d_2\ddot{G}_1(t) + d_2\ddot{G}_2(t)\frac{2}{\beta} - d_1G_3(t)\beta \\ &+ d_9d_{16}G_5(t) + d_{11}d_{16}\ddot{G}_5(t) + d_{11}d_{17}\frac{2}{\beta}\ddot{G}_5(t) + d_9d_{17}\frac{2}{\beta}G_5(t) \\ &+ d_{10}d_{17}\frac{2}{\beta}G_6(t) + d_{10}d_{16}G_6(t) + d_6d_8d_{16}F(r,t) + \frac{2}{\beta}d_6d_8d_{17}F(r,t) \end{aligned} \right\} J_1(\beta r) \\ + \left\{ \begin{aligned} &[(1+d_5)\beta^2G_2(t) - d_2\ddot{G}_2(t) + d_1\beta G_4(t) - d_9d_{17}G_5(t) - d_{11}d_{17}\ddot{G}_5(t)] \\ &- d_{10}d_{17}G_6(t) - d_6d_8d_{17}F(r,t) \end{aligned} \right\} rJ_0(\beta r) = 0 \quad (35)$$

$$\left\{ \begin{aligned} &d_4\beta\dot{G}_1(t) - G_3(t)\beta^2 + d_3\dot{G}_3(t) + 2G_4(t)\beta + d_{14}d_{18}\dot{G}_5(t) \\ &+ d_{13}d_{18}G_6(t) + d_{15}d_{18}\dot{G}_6(t) + d_7d_{12}d_{18}Q(r,t) \end{aligned} \right\} J_0(\beta r) \\ + \left\{ \begin{aligned} &+ d_4\beta\dot{G}_2(t) - G_4(t)\beta^2 + d_3\dot{G}_4(t) + d_7d_{12}d_{19}Q(r,t) \\ &+ d_{14}d_{19}\dot{G}_5(t) + d_{13}d_{19}G_6(t) + d_{15}d_{19}\dot{G}_6(t) \end{aligned} \right\} rJ_1(\beta r) = 0$$

where $d_7 - d_{19}$ are coefficient of H Expansions and presented in appendix.

The guessed functions Eq.(32) can satisfy nonhomogeneous part of Eqs.(6) and (7) if only and if:

$$\begin{aligned} &-(1+d_5)G_1(t)\beta^2 + d_2\ddot{G}_1(t) + d_2\ddot{G}_2(t)\frac{2}{\beta} - d_1G_3(t)\beta + d_9d_{16}G_5(t) + d_{11}d_{16}\ddot{G}_5(t) + d_{11}d_{17}\frac{2}{\beta}\ddot{G}_5(t) \\ &+ d_9d_{17}\frac{2}{\beta}G_5(t) + d_{10}d_{17}\frac{2}{\beta}G_6(t) + d_{10}d_{16}G_6(t) + d_6d_8d_{16}F(r,t) + \frac{2}{\beta}d_6d_8d_{17}F(r,t) = 0 \\ &(1+d_5)\beta^2G_2(t) - d_2\ddot{G}_2(t) + d_1\beta G_4(t) - d_9d_{17}G_5(t) - d_{11}d_{17}\ddot{G}_5(t) - d_{10}d_{17}G_6(t) - d_6d_8d_{17}F(r,t) = 0 \\ &d_4\beta\dot{G}_1(t) - G_3(t)\beta^2 + d_3\dot{G}_3(t) + 2\beta G_4(t) + d_{14}d_{18}\dot{G}_5(t) + d_{13}d_{18}G_6(t) + d_{15}d_{18}\dot{G}_6(t) + d_7d_{12}d_{18}Q(r,t) = 0 \\ &d_4\beta\dot{G}_2(t) - G_4(t)\beta^2 + d_3\dot{G}_4(t) + d_{14}d_{19}\dot{G}_5(t) + d_{13}d_{19}G_6(t) + d_{15}d_{19}\dot{G}_6(t) + d_7d_{12}d_{19}Q(r,t) = 0 \end{aligned} \quad (36)$$

Taking the Laplace transform of Eqs. (36) and using tow boundary conditions of Eqs. (8) (for solid cylinder only the second and forth boundary conditions are applicable), give:

$$\left[\begin{array}{ccccccc} -(1+d_5)\beta^2 + d_2s^2 & d_2s^2\frac{2}{\beta} & -d_1\beta & 0 & d_9d_{16} + d_{11}d_{16}s^2 & & \\ & & & & + d_{11}d_{17}\frac{2}{\beta}s^2 + d_9d_{17}\frac{2}{\beta} & d_{10}d_{17}\frac{2}{\beta} + d_{10}d_{16} & \\ 0 & (1+d_5)\beta^2 - d_2s^2 & 0 & d_1\beta & -d_9d_{17} - d_{11}d_{17}s^2 & -d_{10}d_{17} & \\ d_4\beta s & 0 & -\beta^2 + d_3s & 2\beta & d_{14}d_{18}s & d_{13}d_{18} + d_{15}d_{18}s & \\ 0 & d_4\beta s & 0 & -\beta^2 + d_3s & d_{14}d_{19}s & d_{13}d_{19} + d_{15}d_{19}s & \\ \frac{\{C_{21}J_1(\beta) + C_{22}\{\beta J_0(\beta) - J_1(\beta)\}\}}{s} & 0 & \frac{C_{23}J_0(\beta)}{s} & 0 & 0 & 0 & \\ 0 & 0 & \frac{\{C_{41}J_0(\beta) - C_{42}\beta J_1(\beta)\}}{s} & 0 & 0 & 0 & \end{array} \right] \quad (37)$$

$$\times \begin{bmatrix} G_1(s) \\ G_2(s) \\ G_3(s) \\ G_4(s) \\ G_5(s) \\ G_6(s) \end{bmatrix} = \begin{bmatrix} -d_6d_8d_{16}F(r,s) - \frac{2}{\beta}d_6d_8d_{17}F(r,s) \\ d_6d_8d_{17}F(r,s) \\ -d_7d_{12}d_{18}Q(r,s) \\ -d_7d_{12}d_{19}Q(r,s) \\ f_2(s) \\ f_4(s) \end{bmatrix}$$

Eqs. (37) is a system of algebraic equations and is solved for $G_{1n}(t)$ to $G_{6n}(t)$ by the Cramer methods in the Laplace domain where by the inverse Laplace transform the function are transformed into the real time domain. In the process of solution, it is necessary to consider the following points.

- 1-The initial conditions Eq.(9) are considered only for general solutions Eq.(31) . The initial conditions of $G_{1n}(t) - G_{6n}(t)$ for the particular solutions are considered equal to zero.
- 2-Eq. (37) is in polynomial form function of the Laplace parameters s (not Bessel functions form of s). Therefore the exact inverse Laplace transforms is possible and somehow simple.
- 3-For hollow cylinder, it is enough to include the second type of Bessel functions $Y(r)$ in the sequence of particular solution as [22-28]:

$$\begin{aligned} u^p(r,t) &= \sum_{n=1}^{\infty} \{ [G_{1n}(t)J_1(\beta_n r) + G_{2n}(t)rJ_2(\beta_n r)] + [G_{3n}(t)Y_1(\beta_n r) + G_{4n}(t)rY_2(\beta_n r)] \} + rG_{5n}(t) + r^2 G_{6n}(t) \\ T^p(r,t) &= \sum_{n=1}^{\infty} \{ [G_{7n}(t)J_0(\beta_n r) + G_{8n}(t)rJ_1(\beta_n r)] + [G_{9n}(t)Y_0(\beta_n r) + G_{10n}(t)rY_1(\beta_n r)] \} + rG_{11n}(t) + r^2 G_{12n}(t) \end{aligned} \quad (38)$$

Substituting Eqs. (38) in Eqs. (6) and (7), eight equations are obtained where using the four boundary conditions Eq.(8), 12 functions $G_{1n}(t) - G_{12n}(t)$ are obtained for the hollow cylinder.

4 RESULTS AND DISCUSSIONS

As an example, a solid cylinder with $r_o = 1m$ made of aluminium is considered. The material properties are shown in Table1.[7,22-23]:

Table 1

The initial temperature T_o is considered 293° K.

Material properties of Aluminum
E=70 (G Pa)
$\nu = 0.3$
$\alpha = 23 \times 10^{-6}$ (1 / K)
$\rho = 2707$ (kg / m ³)
K=204(W/m K)
c=903(J/kg K)
$H_z = 5 \times 10^8$ (A / m) Hz=0 &

Now, an instantaneous hot outside surface temperature $T(1,t) = 10^{-3}T_o\delta(t)$ where $\delta(t)$ is the unit Dirac function, is considered, and the outside radius of the cylinder is assumed to be fixed ($u(1,t) = 0$). To draw the graphs, a nondimensional time $\hat{t} = \frac{vt}{r}$ is considered, where $v = \sqrt{E(1-\nu) / \rho(1+\nu)(1-2\nu)}$ is the dilatational-wave velocity [31-35].

Figs. 2 - 5 show the wave fronts of displacement, temperature, radial and hoop stress with and without magnetic field at $\hat{t} = 0.2$.

As a second example, a mechanical shock wave of the form $u(1,t) = 10^{-12}u_o\delta(t)$ is applied to the outside surface of the cylinder, where the surface is assumed to be at zero temperature ($T(1,t) = 0$) and ($u_o = r_o\alpha T_o$) is an assumed initial displacement at $\hat{t} = 0.6$.

These figures show the magnetic field increases the stiffness of body and then decreases the temperature and displacement. Figs. 6 - 9 show the wave fronts for the displacement, temperature, radial and hoop stress with and without magnetic field distributions along the radial direction. The convergence of the solutions for these examples is achieved by consideration of 1200 eigenvalues used for the H-Fourier expansion. More than this number of eigenvalues results in the increased round-off and truncation errors, which affect the quality of the graphs. The convergence of solution is faster for displacement in comparison with the temperature. The small oscillations in Figs. 2 and 4 are due to the convergence of solutions.

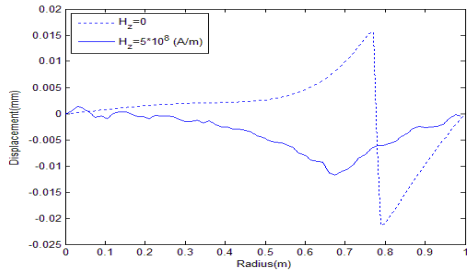


Fig.2
Non-dimensional displacement distribution due to input $T(1,t) = 10^{-3}T_0\delta(t)$ at non-dimensional time $\hat{t} = 0.2$ with and without magnetic field.

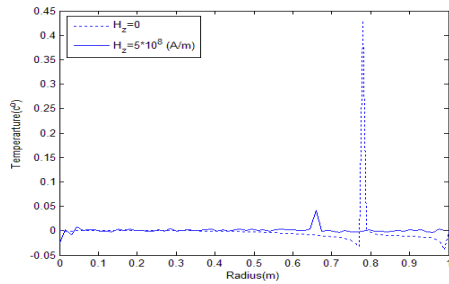


Fig.3
Non-dimensional temperature distribution due to input $T(1,t) = 10^{-3}T_0\delta(t)$ at non-dimensional time $\hat{t} = 0.2$ with and without magnetic field.

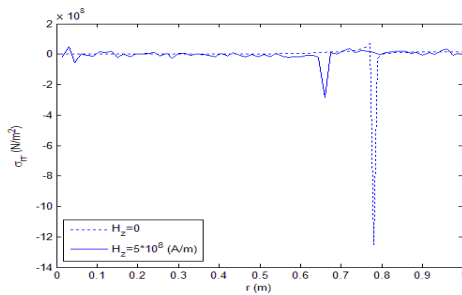


Fig.4
Non-dimensional radial stress distribution due to input $T(1,t) = 10^{-3}T_0\delta(t)$ at non-dimensional time $\hat{t} = 0.2$ with and without magnetic field.

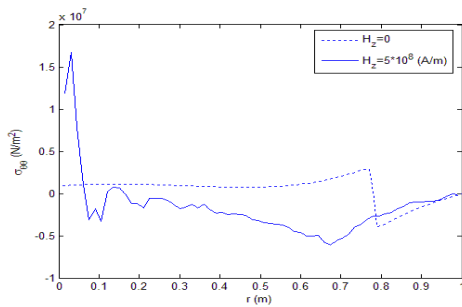


Fig.5
Non-dimensional hoop stress distribution due to input $T(1,t) = 10^{-3}T_0\delta(t)$ at non-dimensional time $\hat{t} = 0.2$ with and without magnetic field.

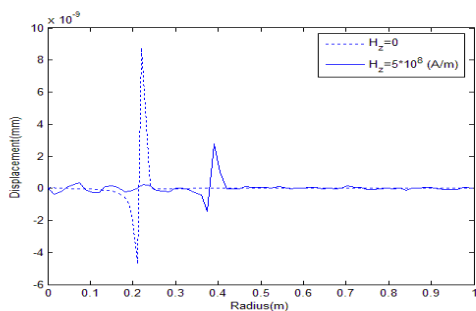
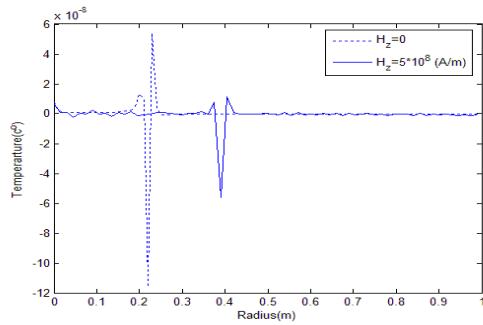
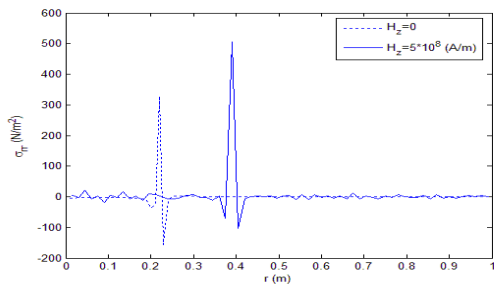


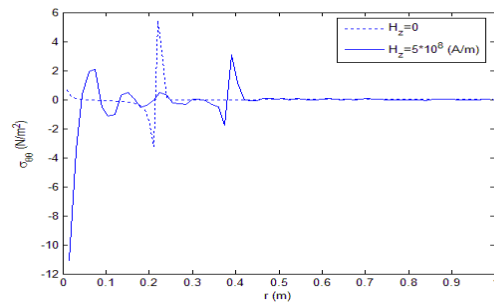
Fig.6
Non-dimensional displacement distribution due to input $u(1,t) = 10^{-12}u_0\delta(t)$ at non-dimensional time $\hat{t} = 0.6$ with and without magnetic field.

**Fig.7**

Non-dimensional temperature distribution due to input $u(1,t) = 10^{-12} u_0 \delta(t)$ at non-dimensional time $\hat{t} = 0.6$ with and without magnetic field .

**Fig.8**

Non-dimensional radial stress distribution due to input $u(1,t) = 10^{-12} u_0 \delta(t)$ at non-dimensional time $\hat{t} = 0.6$ with and without magnetic field .

**Fig.9**

Non-dimensional hoop stress distribution due to input $u(1,t) = 10^{-12} u_0 \delta(t)$ at non-dimensional time $\hat{t} = 0.6$ with and without magnetic field.

5 CONCLUSIONS

In this paper, an analytical solution for the coupled Magneto-thermo-elasticity of thick cylinders under radial temperature or mechanical shock load with and without magnetic field is presented. The method is based on the eigenfunction Fourier expansion, which is a classical and traditional method of solution for the typical initial and boundary value problems. The strength of this method is its ability to reveal the fundamental mathematical and physical properties and the interpretations of the problem under study.

In the coupled Magnetothermoelastic problem of the radial-symmetric cylinder, the governing equations are a system of partial differential equations with two independent variables, the radius (r) and the time (t). The traditional procedure to solve this class of problems is to eliminate the time variable by using the Laplace transform.

The resulting system is a set of ordinary differential equations in terms of the radius variable, which falls into the Bessel function family. This method of analysis brings the Laplace parameter (s) in the argument of the Bessel functions, causing hardship or complications in carrying out the exact inverse of the Laplace transformation. As a result, the numerical inverse of the Laplace transformation is used in the papers dealing with this type of problems in literature. In the present paper, to prevent this problem, when the Laplace transform is applied to the particular solutions, it is postponed after eliminating the radius variable r by the H-Fourier expansion. Thus, the Laplace parameter (s) appears in polynomial function forms, and hence the exact Laplace inversion transformations are possible.

The method described in this paper is an exact solution of the coupled Magneto-thermo-elasticity of thick cylinders with two given boundary conditions. The exact solutions found in literature for the coupled thermoelasticity problems are limited to the infinite spaces and half-spaces. The analytical method of solution presented in this paper is for a finite domain with specified and given boundary conditions. This is the novelty of the paper, where the solution of a popular structural component (a thick cylinder) with two specified boundary conditions under the coupled Magneto-thermo-elasticity assumption is given analytically and in terms of the series solution.

Appendix

$$\begin{aligned}
 d_1 &= -\alpha \frac{(1+\nu)}{(1-\nu)} & d_2 &= -\rho \frac{(1+\nu)(1-2\nu)}{E(1-\nu)} & d_3 &= -\frac{\rho c}{k} & d_4 &= -\frac{E\alpha}{k(1-2\nu)}T_0 \\
 d_5 &= \frac{(1+\nu)(1-2\nu)}{(1-\nu)E} \mu H_z^2 & d_6 &= \frac{(1+\nu)(1-2\nu)}{E(1-\nu)} & d_7 &= \frac{1}{k} & d_8 &= 1 \\
 d_9 &= 3(1+d_5) & d_{10} &= 2rd_1 & d_{11} &= d_2r^2 & d_{12} &= 1 & d_{13} &= 4 \\
 d_{14} &= 3d_4r & d_{15} &= d_3r^2 & d_{16} &= C_0 & d_{17} &= C_1 & d_{18} &= E_0 & d_{19} &= E_1
 \end{aligned}$$

$$\zeta_1 = \left(-(-\beta^2 + \lambda^2 b) / a - \lambda d / (-\beta^2 + \lambda c) \right) / \left(2\lambda^2 b / (a\beta^2) - 2(\beta^2 - \lambda^2 b) / a / (-\beta^2 + \lambda c) \right)$$

$$\zeta_2 = (-\beta_1^2 + \lambda^2 b) / a\beta_1$$

$$\zeta_3 = \left((-\beta^2 + \lambda^2 b) / a\beta + 2\lambda^2 b\zeta_1 / \beta^2 / a \right)$$

$$\zeta_4 = -\frac{1}{2\beta} \left(\lambda d\beta + (-\beta^2 + \lambda c) \left((-\beta^2 + \lambda^2 b) / a\beta + 2\lambda^2 b\zeta_1 / \beta^2 / a \right) \right)$$

$$\mu_{11} = C_{11}J_1(\beta r_i) + C_{12} \left(\beta J_0(\beta r_i) - \frac{1}{r} J_1(\beta r_i) \right) + C_{13}\zeta_2 J_0(\beta r_i)$$

$$\mu_{12} = C_{11} \left(J_1(\beta r_i) + \zeta_1 r_i J_2(\beta r_i) \right) + C_{12} \left(\beta J_0(\beta r_i) - \frac{1}{r_i} J_1(\beta r_i) + \zeta_1 J_2(\beta r_i) + \zeta_1 r_i \beta J_1(\beta r_i) - 2\zeta_1 J_2(\beta r_i) \right)$$

$$+ C_{13} \left(\zeta_3 J_0(\beta r_i) + \zeta_4 r_i J_1(\beta r_i) \right)$$

$$\mu_{13} = C_{11}Y_1(\beta r_i) + C_{12} \left(\beta Y_0(\beta r_i) - \frac{1}{r} Y_1(\beta r_i) \right) + C_{13}\zeta_2 Y_0(\beta r_i)$$

$$\mu_{14} = C_{11} \left(Y_1(\beta r_i) + \zeta_1 r_i Y_2(\beta r_i) \right) + C_{12} \left(\beta Y_0(\beta r_i) - \frac{1}{r_i} Y_1(\beta r_i) + \zeta_1 Y_2(\beta r_i) + \zeta_1 r_i \beta Y_1(\beta r_i) - 2\zeta_1 Y_2(\beta r_i) \right)$$

$$C_{13} \left(\zeta_3 Y_0(\beta r_i) + \zeta_4 r_i Y_1(\beta r_i) \right)$$

$$\mu_{21} = C_{21}J_1(\beta r_o) + A_1 C_{22} \left(\beta J_0(\beta r_o) - \frac{1}{r_o} J_1(\beta r_o) \right) + C_{23}\zeta_2 J_0(\beta r_o)$$

$$\mu_{22} = C_{21} \left(J_1(\beta r_o) + \zeta_1 r_o J_2(\beta r_o) \right) + C_{22} \left(\beta J_0(\beta r_o) - \frac{1}{r_o} J_1(\beta r_o) + \zeta_1 J_2(\beta r_o) + \zeta_1 r_o \beta J_1(\beta r_o) - 2\zeta_1 J_2(\beta r_o) \right)$$

$$C_{23} \left(\zeta_3 J_0(\beta r_o) + \zeta_4 r_o J_1(\beta r_o) \right)$$

$$\begin{aligned} \mu_{23} &= C_{21} Y_1(\beta r_o) + C_{22} \left(\beta Y_0(\beta r_o) - \frac{1}{r_o} Y_1(\beta r_o) \right) + C_{23} \zeta_2 Y_0(\beta r_o) \\ \mu_{24} &= C_{21} \left(Y_1(\beta r_o) + \zeta_1 r_o Y_2(\beta r_o) \right) + C_{22} \left(\beta Y_0(\beta r_o) - \frac{1}{r_o} Y_1(\beta r_o) + \zeta_1 Y_2(\beta r_o) + \zeta_1 r_o \beta Y_1(\beta r_o) - 2\zeta_1 Y_2(\beta r_o) \right) \\ &+ C_{23} \left(\zeta_3 Y_0(\beta r_o) + \zeta_4 r_o Y_1(\beta r_o) \right) \\ \mu_{31} &= C_{31} \zeta_2 J_0(\beta r_i) - C_{32} \zeta_2 \beta J_1(\beta r_i) \\ \mu_{32} &= C_{31} \left(\zeta_3 J_0(\beta r_i) + \zeta_4 r_i J_1(\beta r_i) \right) + C_{32} \left(-\zeta_3 \beta J_1(\beta r_i) + \zeta_4 J_1(\beta r_i) + \zeta_4 r_i \beta J_0(\beta r_i) - \zeta_4 J_1(\beta r_i) \right) \\ \mu_{33} &= C_{31} \zeta_2 Y_0(\beta r_i) - C_{32} \zeta_2 \beta Y_1(\beta r_i) \\ \mu_{34} &= C_{31} \left(\zeta_3 Y_0(\beta r_i) + \zeta_4 r_i Y_1(\beta r_i) \right) + C_{32} \left(-\zeta_3 \beta Y_1(\beta r_i) + \zeta_4 Y_1(\beta r_i) + \zeta_4 r_i \beta Y_0(\beta r_i) - \zeta_4 Y_1(\beta r_i) \right) \\ \mu_{41} &= \left(C_{41} \zeta_2 J_0(\beta r) - C_{42} \zeta_2 \beta J_1(\beta r_o) \right) A_1 \\ \mu_{42} &= C_{41} \left(\zeta_3 J_0(\beta r) + \zeta_4 r J_1(\beta r) \right) + C_{42} \left(-\zeta_3 \beta J_1(\beta r_o) + \zeta_4 J_1(\beta r_o) + \zeta_4 r_o \beta J_0(\beta r_o) - \zeta_4 J_1(\beta r_o) \right) \\ \mu_{43} &= C_{41} \zeta_2 Y_0(\beta r) - C_{42} \zeta_2 \beta Y_1(\beta r_o) \\ \mu_{44} &= C_{41} \left(\zeta_3 Y_0(\beta r) + \zeta_4 r Y_1(\beta r) \right) + C_{42} \left(-\zeta_3 \beta Y_1(\beta r_o) + \zeta_4 Y_1(\beta r_o) + \zeta_4 r_o \beta Y_0(\beta r_o) - \zeta_4 Y_1(\beta r_o) \right) \end{aligned}$$

REFERENCES

- [1] Hetnarski R. B., 1964, Solution of the coupled problem of thermoelasticity in the form of series of functions, *Archivum Mechaniki Stosowanej* **16**:919-941.
- [2] Hetnarski R.B., Ignaczak J., 1993, Generalized Thermoelasticity: Closed-Form Solutions, *Journal of Thermal Stresses* **16**: 473-498.
- [3] Hetnarski R.B., Ignaczak J., 1994, Generalized Thermoelasticity: Response of Semi-Space to a Short Laser Pulse, *Journal of Thermal Stresses* **17**:377-396.
- [4] Georgiadis H. G., Lykotrafitis G., 2005, Rayleigh Waves Generated by a Thermal Source: A Three-dimensional Transient thermoelasticity Solution, *Journal of Applied Mechanics* **72**:129-138.
- [5] Wagner P., 1994, Fundamental Matrix of the System of Dynamic Linear Thermoelasticity, *Journal of Thermal Stresses* **17**:549-565.
- [6] Lee Z.Y., 2009, Magneto thermoelastic analysis of multilayered conical shells subjected to magnetic and vapor fields, *International Journal of Thermal Sciences* **48**:50-72.
- [7] Dai H.L., Fu Y.M., 2007, Magneto thermoelastic interactions in hollow structures of functionally graded material subjected to mechanical loads, *International Journal of Pressure Vessels and Piping* **84**:132-138.
- [8] Wang X., Dong K., 2006, Magneto thermodynamic stress and perturbation of magnetic field vector in a non-homogeneous thermoelastic cylinder, *European Journal of Mechanics - A/Solids* **25**:98-109.
- [9] Dai H.L., X. Wang, 2006, The dynamic response and perturbation of magnetic field vector of orthotropic cylinders under various shock loads, *International Journal of Pressure Vessels and Piping* **83**:55-62.
- [10] Misra S. C., Samanta S. C., Chakrabarti A. K., 1992, Transient magneto thermoelastic waves in a viscoelastic half-space produced by ramp-type heating of its surface, *Computers & Structures* **43**:951-957.
- [11] Massalas C. V., 1991, A note on magneto thermoelastic interactions, *International Journal Engineering Science* **29**:1217-1229.
- [12] Misra J. C., Samanta S. C., Chakrabarti A. K., Misra Subhas C., 1991, Magneto thermoelastic interaction in an infinite elastic continuum with a cylindrical hole subjected to ramp-type heating, *International Journal Engineering Science* **29**: 1505-1514.
- [13] Roy Choudhuri S. K., Chatterjee Roy G., 1990, Temperature-rate dependent magneto thermoelastic waves in a finitely conducting elastic half-space, *Journal Computers & Mathematics with Applications* **19**:85-93.
- [14] H. S., Narasimhan R., 1987, Magneto thermoelastic stress waves in a circular cylinder, *International Journal of Engineering Science*, **25**: 413-425.
- [15] Gargi Chatterjee(Roy), Roychoudhuri S. K., 1985, The coupled magneto thermoelastic problem in elastic half-space with two relaxation times, *International Journal Engineering Science* **23**: 975-986.
- [16] Maruszewski B., 1981, Dynamical magneto thermoelastic problem in circular cylinders-I: Basic equations, *International Journal Engineering Science* **19**:1233-1240.
- [17] Ezzat M. A., El-Karamany A. S., 2003, Magneto thermoelasticity with two relaxation times in conducting medium with variable electrical and thermal conductivity, *Journal Applied Mathematics and Computation* **142**:449-467.

- [18] Chen W.Q., Lee K.Y., 2003, Alternative state space formulations magnetoelastic thermoelasticity with transverse isotropy and the application to bending analysis of nonhomogeneous plates, *Journal Solids & Structures* **40**: 5689-5705.
- [19] Tianhu H., Yapeng S., Xiaogeng T., 2004, A two-dimensional generalized thermal shock problem for a half-space in electromagneto-thermoelasticity, *International Journal Engineering. Science* **42**:809-823.
- [20] Sharma J.N., Pal M., 2004, Rayleigh-Lamb waves in magneto thermoelastic homogeneous isotropic plate, *International Journal Engineering Science* **42**:137-155.
- [21] Abd-Alla A.M., Hammad H.A.H., Abo-Dahab S.M., 2004, Magneto-thermo-viscoelastic interactions in an unbounded body with a spherical cavity subjected to a periodic loading, *Journal Applied Mathematics and Computation* **155**:235-248.
- [22] Jabbari M., Dehbani H., Eslami MR., 2010, An Exact Solution for Classic Coupled Thermo elasticity in Spherical Coordinates, *Journal of Pressure Vessel, ASME, Transaction* **132**: 031201-11.
- [23] Jabbari M., Dehbani H., Eslami MR., 2011, An Exact Solution for Classic Coupled Thermo elasticity in Cylindrical Coordinates, *Journal of Pressure Vessel, ASME, Transaction* **133**: 051204-10.
- [24] Jabbari M., Dehbani H., 2009, An Exact Solution for Classic Coupled Thermoporoelasticity in Cylindrical Coordinates, *Journal of Solid Mechanics* **1**: 343-357.
- [25] Jabbari M., Dehbani H., 2010, An Exact Solution for Classic Coupled Thermoporoelasticity in Ax symmetric Cylinder, *Journal of Solid Mechanics* **2**: 129-143.
- [26] Jabbari M., Dehbani H., 2010, An Exact Solution for Lord-Shulman Generalized Coupled Thermo poroelasticity in Spherical Coordinates, *Journal of Solid Mechanics* **2**: 214-230.
- [27] Jabbari M., Dehbani H., 2011, An Exact Solution for Lord-Shulman Generalized Coupled Thermoporoelasticity in Cylindrical Coordinates, Published in 9th international congress on thermal, Budapest, Hungry.
- [28] Jabbari M., Dehbani H., 2012, An Exact Solution for Quasi-Static Poro-Thermoelasticity in Spherical Coordinates, *Iranian journal of mechanical engineering transactions of the ISME* **12**: 86-108.
- [29] Necati Ozisik M., 1980, Heat conduction, Wiley & Sons.
- [30] Hetnarski R. B., Eslami M. R., 2009, Thermal Stresses Advanced Theory and Applications, Springer, New York..
- [31] Berezovski A., Engelbrecht J., Maugin G. A., 2003, Numerical Simulation of Two-Dimensional Wave Propagation in Functionally Graded Materials, *Eur. J. Mech. A/Solids* **22**: 257–265.
- [32] Berezovski A., Maugin G. A., 2003, Simulation of Wave and Front Propagation in Thermoelastic Materials With Phase Transformation, *Comput. Mater. Sci* **28**: 478–485.
- [33] Berezovski A., Maugin G. A., 2001, Simulation of Thermoelastic Wave Propagation by Means of a Composite Wave-Propagation Algorithm, *J.Comput. Phys* **168**: 249–264.
- [34] Engelbrecht J., Berezovski A., Saluperea A., 2007, Nonlinear Deformation Waves in Solids and Dispersion, *Wave Motion* **44**: 493–500.
- [35] Angel Y. C., Achenbach J. D., 1985, Reflection and Transmission of Elastic Waves by a Periodic Array of Cracks: Oblique Incidence, *Wave Motion* **7**: 375–397.